APPLIED GEOPHYSICS, Vol.21, No.4 (December 2024), P. 1–11, 8 Figures.
DOI:10.1007/s11770-024-1113-8

Characteristics of secondary microseisms generated in the Bohai Sea and their impact on seismic noise

Yin Kang-Da[1,2*], Zhang Xiao-Gang[1,2], Li Xiao-Jun[1,2], Mao Guo-Liang[1,2], Zhang Xing-Xing[1,2], and Jia Xiao-Hui[3]

Abstract: In this study, we use the Bohai Sea area as an example to investigate the characteristics of secondary microseisms and their impact on seismic noise based on the temporal frequency spectral analysis of observation data from 33 broadband seismic stations during strong gust periods, and new perspectives are proposed on the generation mechanisms of secondary microseisms. The results show that short-period double-frequency (SPDF) and long-period double-frequency (LPDF) microseisms exhibit significant alternating trends of strengthening and weakening in the northwest area of the Bohai Sea. SPDF microseisms are generated by irregular wind waves during strong offshore wind periods, with a broad frequency band distributed in the range of 0.2–1 Hz; LPDF microseisms are generated by regular swells during periods of sea wind weakening, with a narrow frequency band concentrated between 0.15 and 0.3 Hz. In terms of temporal dimensions, as the sea wind weakens, the energy of SPDF microseisms weakens, and the dominant frequencies increase, whereas the energy of LPDF microseisms strengthens and the dominant frequencies decrease, which is consistent with the process of the decay of wind waves and the growth of swells. In terms of spatial dimensions, as the microseisms propagate inland areas, the advantageous frequency band and energy of SPDF microseisms are reduced and significantly attenuated, respectively, whereas LPDF microseisms show no significant changes. And during the propagation process in high-elevation areas, LPDF microseisms exhibit a certain site amplification effect when the energy is strong. The results provide important supplements to the basic theory of secondary microseisms, preliminarily reveal the relationship between the atmosphere, ocean, and seismic noise, and provide important theoretical references for conducting geological and oceanographic research based on the characteristics of secondary microseisms.
Keywords: Secondary microseisms, seismic noise, temporal frequency spectral analysis, generation mechanisms, site amplification effect

Introduction

Seismic noise is an important indicator for measuring the observation level and data quality of a seismic station (Sleeman and Vila, 2007; Lin et al., 2020). Long-period natural noise and high-frequency artificial noise are the main sources of seismic noise (Ge et al., 2013). The Earth's motion caused by the transformation of atmospheric pressure produces background noise in the period range of 20–100 s (Sorrells and Douze, 1974); the shallow sea coast produces primary microseisms in the period range of 10–20 s driven by wave pressure (Hasselmann, 1963); two primary microseisms with the

Manuscript received by the Editor March 28, 2024; revised manuscript received June 3, 2024.
1. Hebei Earthquake Agency, Shijiazhuang 050021, China.
2. Hebei Hongshan National Observatory on Thick Sediments and Seismic Hazards, Xingtai 054000, China.
3. School of Urban Geology and Engineering, Hebei GEO University, Shijiazhuang 050031, China.
*Corresponding author: Yin Kang-Da (Email: yinkangda@126.com).

same frequency and opposite directions near the coast nonlinearly interact to produce secondary microseisms in the period range of 5–10 s (Longuet-Higgins, 1950); noise above 1 Hz is primarily related to cultural activities (Cupillard and Capdeville, 2010; Wang et al., 2011).

Oceanic microseisms are important sources of seismic noise with the characteristics of wide frequency band, high energy, and wide impact area. Because of the complex energy transfer and coupling between the atmosphere, ocean, and solid Earth, the study of the generation mechanisms of oceanic microseisms has been listed as one of the ten seismological grand challenges (Lay et al., 2009; Zheng et al., 2017; Chen et al., 2018). Based on the coupling relationship between ocean waves and Earth's microseisms, ocean processes can be monitored, and it also provides novel methods for exploring the internal structure of the Earth (Lay et al., 2009; Wei et al., 2020). Wei et al. (2022) conducted a study on the anomalies of secondary microseisms before earthquakes, which provided a possibility for earthquake prediction based on the characteristics of secondary microseisms.

Seismologists and oceanographers have conducted extensive research on the theory of oceanic microseisms. Based on their frequency band range and generation mechanisms, oceanic microseisms can be divided into primary and secondary microseisms. Primary microseisms, also known as single-frequency microseisms, are produced by ocean waves interacting with the coast or seafloor at frequencies mainly distributed between 0.05 and 0.12 Hz. Secondary microseisms, also known as double-frequency microseisms, are produced by stationary waves generated by the interaction between ocean waves traveling at similar frequencies in opposite directions (Longuet-Higgins, 1950; Hasselmann, 1963; Zheng et al., 2017). Multiple studies (Lepore and Grad, 2020; Lepore and Grad, 2018; Bromirski et al., 2005; Koper and Burlacu, 2015; Xiao et al., 2018) have shown that secondary microseisms occasionally split into SPDF microseisms in the range of 0.25–0.8 Hz and LPDF microseisms in the range of 0.1–0.25 Hz and attributed this phenomenon primarily to nonlinear interactions between strong wind waves traveling from different oceans in the open sea, which propagate to the shore.

These results are mostly based on open sea areas. However, the Bohai Sea, as the inland sea of China, penetrates deep into the land and is only connected to the open sea through a narrow strait. The characteristics of secondary microseisms generated in the Bohai Sea and their impact on seismic noise in inland areas need to be further studied. Therefore, based on previous studies, we selected observation data from seismic stations during strong gust periods in the Bohai Sea to analyze the characteristics of secondary microseisms and their variation with the wind process using the temporal frequency spectral method. Combined with the special geographical location and wave characteristics of the Bohai Sea, the generation mechanisms of secondary microseisms were studied in depth.

Data and methods

We selected observation data from 33 broadband surface rock seismic stations in the northwest inland area of the Bohai Sea during strong gust periods from November 3 to 7, 2023. Broadband seismometers have lower self-noise levels and larger dynamic ranges (Sleeman et al., 2006; Li et al., 2015), which can reduce measurement errors caused by instrument factors and obtain more reliable observation data. The distribution of seismic stations is shown in Figure 1. The variation curve of the ocean surface stress equivalent 10 m neutral wind speed at the red box is shown in Figure 2. The wind speed monitoring location is approximately 14 km from the coastline, and the wind speed data are sourced from historical reanalysis datasets from the European Centre for Medium-Range Weather Forecasts (ECMWF).

Power spectral density

Seismic noise is generally a stationary and random vibration process, and the power spectral density (PSD) is a general method for quantitatively analyzing seismic noise in the frequency domain (Xu and Yuan, 2019; Yang et al., 2019). We selected 120 hours of consecutive observation data from 33 stations, as shown in Figure 1, from November 3 to 7 for research and calculated the PSDs of the vertical components for each hour to analyze the temporal frequency spectra. Because the linear trend offsets the spectrum energy in the low-frequency band, resulting in significant distortion in the spectrum estimation (McNamara and Buland, 2004), all records are preprocessed using mean and trend removal before the PSD calculation.

The Welch method (Welch, 1967) was used for PSD calculations. The basic idea is to divide the original

record into segments of equal length and adjacent segments can overlap with each other. The PSD results of all segments are averaged to improve the accuracy of the spectral estimation. The PSD calculation process refers to the parameters in McNamara and Buland (2004). The 1-h record was divided into 13 segments with an overlap rate of 75%, and the Hanning window was selected as the window function.

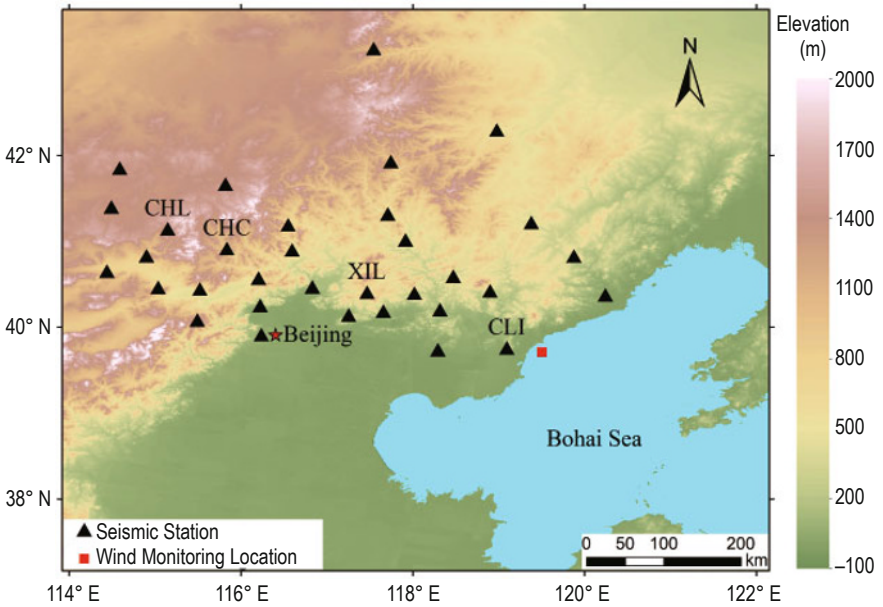

Figure 1. Distribution of seismic stations in the northwest inland area of the Bohai Sea. The red box represents the monitoring location of wind speed in the Bohai Sea, and the black triangles represent seismic stations.

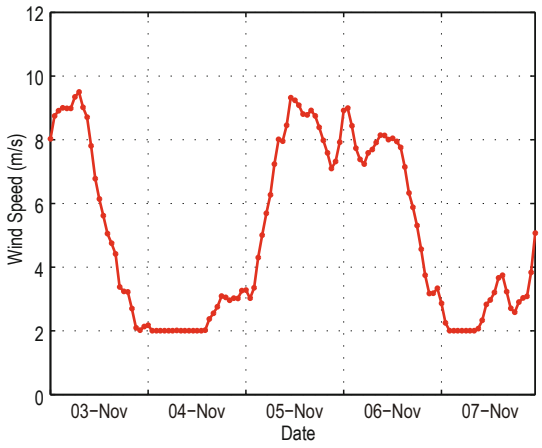

Figure 2. Variation in ocean surface stress equivalent 10 m neutral wind speed from November 3 to 7, 2023.

Smoothing of PSD curves

To avoid the randomness of the results and the existence of outliers, the PSD curves were smoothed using the octave method in McNamara and Buland (2004) and Xie et al. (2018). According to the 1/16 octave, 54 center frequencies with equal intervals in logarithmic coordinates and 54 sub-bands in the range of 0.1–1 Hz were obtained using Equation (1). To ensure sufficient sampling of the record and the overlap of sub-bands, the width of the sub-band was taken as 1/8 octave. We used the average power of each band to represent the level of noise at the center frequency.

$$f_m = 2^{(m-1)/16} f_0, \tag{1}$$

where f_m denotes the center frequency, m=1,⋯,54, and f_0 takes the value of 0.1 Hz.

f_1 and f_2, defined in Equations (2) and (3), respectively, denote the lower and upper cut-off frequencies of each 1/8 octave sub-band, with f_m as the center frequency.

$$f_1 = 2^{-1/16} f_m, \tag{2}$$

$$f_2 = 2^{1/16} f_m. \tag{3}$$

Probability density function

The probability density function (PDF) is the probability distribution statistic of many smoothed PSD curves over long-time scales, which can comprehensively evaluate the variation characteristics of seismic noise. The PDF at the center frequency f_m can be expressed using the following equation (McNamara and Buland, 2004; Wu et al., 2012; Guo et al., 2023):

$$\mathrm{P}(f_m) = N_{Pf_m}/N_{f_m}, \tag{4}$$

where N_{Pf_m} denotes the number of PSD curves that fall

within each PSD unit interval, and N_{f_m} denotes the total number of PSD curves at the center frequency f_m.

Results and discussion

PSD analysis in terms of temporal dimensions

First, four stations (CLI, XIL, CHC, and CHL) at different distances from the coastline were selected for temporal frequency spectral analysis. The geographical locations of the four stations are shown in Figure 1. Basic information about the stations is presented in Table 1. By arranging the seismic noise PSD curves of the four stations along the time axis from November 3 to 7 (Figure 3), the variation regularity of secondary microseisms with the sea wind process was analyzed using the temporal frequency spectral method. According to Figure 3, with the variation in wind speed (black dashed lines), the seismic noise levels at the four stations exhibit strong fluctuations in the frequency range of 0.1–1 Hz, with the energy concentrated in the wider frequency band between 0.2 and 1 Hz and the narrow frequency band between 0.15 and 0.3 Hz, which correspond to the SPDF and LPDF microseisms mentioned in previous studies, e.g., Lepore and Grad (2020). During the strong wind periods on November 3, 5, and 6, the energy of SPDF microseisms was high, whereas that of LPDF microseisms was weak. However, during the weak wind periods on November 4 and 7, the energy of SPDF microseisms significantly weakened, whereas that of LPDF microseisms significantly strengthened. Overall, with the process of sea wind action, the energies of SPDF and LPDF microseisms exhibit significant alternating trends of strengthening and weakening.

Compared with station CLI, the energy and advantageous frequency band of SPDF microseisms at the other stations (XIL, CHC, and CHL) further away from the coastline decreased significantly during the strong wind periods on November 3, 5, and 6, mainly

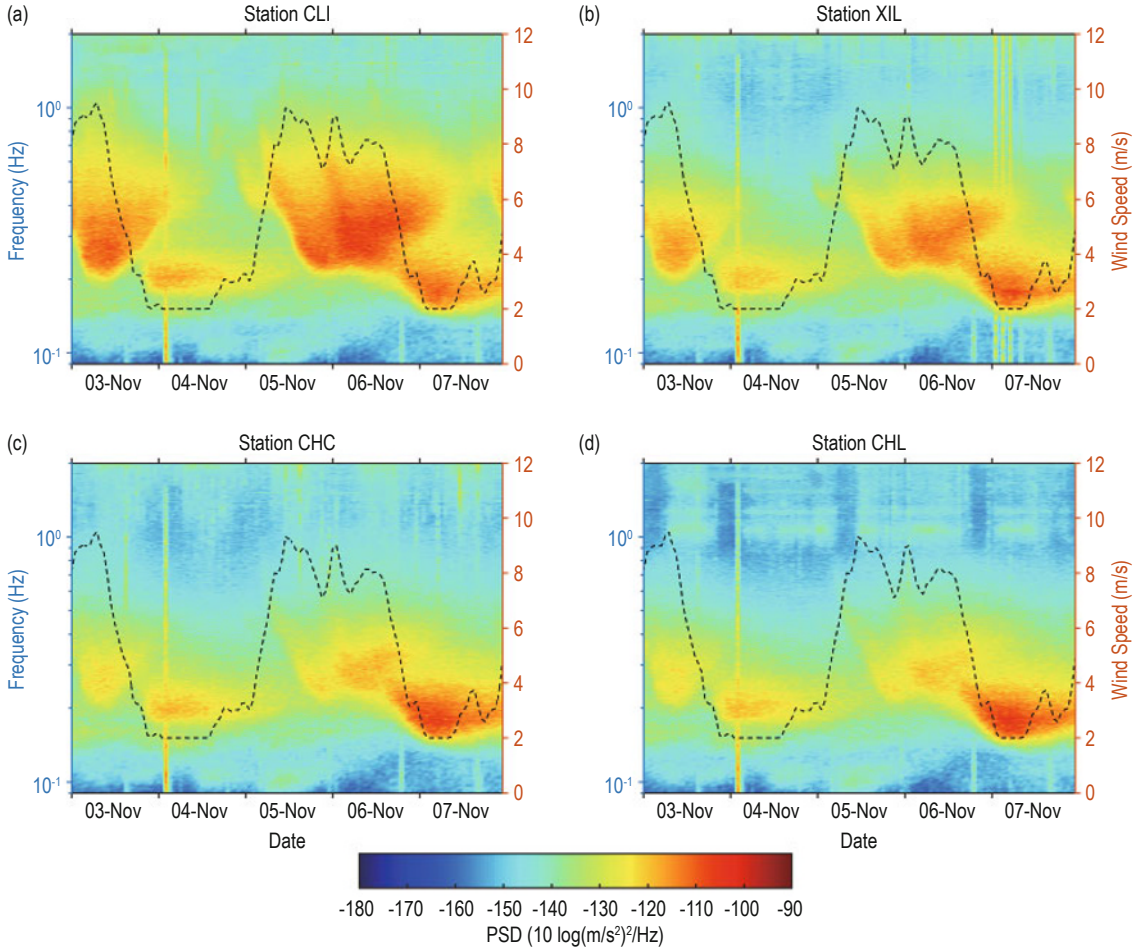

Figure 3. Temporal frequency spectrograms of seismic noise recorded at stations (a) CLI, (b) XIL, (c) CHC, and (d) CHL from November 3 to 7, 2023. The black dashed lines represent the variation in wind speed.

because of the fast attenuation of high-frequency signals during their propagation inland. During the weak wind periods on November 4 and 7, no significant energy attenuation of LPDF microseisms occurred, nor did the advantageous frequency band change significantly.

Table 1 Basic station information.

Station	Data logger	Seismometer	Frequency band	Lithology	Elevation (m)
CLI	REF TEK Wrangler	Güralp 3T	120s–50Hz	Granite	61
XIL	EDAS-24IP	BBVS-60	60s–50Hz	Limestone	604
CHC	EDAS-24IP	BBVS-60	60s–50Hz	Gneiss	884
CHL	REF TEK Wrangler	Trillium Horizon 360	360s–136Hz	Granite	1339

Oceanic microseisms are generated by wave activity, and most waves are generated by the action of wind, mainly wind waves and swells. Wind waves are rapid waves with varying heights and lengths generated by the direct action of sea wind. Wave surfaces are steep and rough, with short periods that vary significantly with sea wind. Swells refer to waves in areas where the wind stops, or the wind speed and direction change suddenly, and wind waves leave the wind area. They are neatly arranged, with smooth wave surfaces, and the periods are long and concentrated (Wiegel, 1960; Wang et al., 1990; Guo et al., 1997; Hwang et al., 2012). Because of the special geographical location of the Bohai Sea, waves from the open sea are not easily propagated into the interior, and the growth of internal waves is also limited by the terrain. The sea area is primarily dominated by wind waves, and the swells are mostly generated by wind waves after the reduction of sea wind (Niu et al., 1999; Yin and Zhang, 2006). The results of Sun (1991) show that pure wind waves in the western Bohai Sea account for 66.8%, mixed waves mainly composed of swells account for 29% and mixed waves mainly composed of wind waves account for 4.2%. Strong wind is the main factor in generating waves. The variation regularity of secondary microseisms shown in Figure 3 is consistent with the sea wind process and the generation mechanisms and characteristics of wind waves and swells in the Bohai Sea. In other words, during strong wind periods, the sea area is primarily dominated by irregular and short-period wind waves, whereas during weak wind periods, the sea area is primarily dominated by more regular and long-period swells.

Figure 4 shows the variation in seismic noise PSD curves of stations CLI and CHL with significant differences in the distance from the coastline between 0.1 and 1 Hz during the period of sea wind strengthening from 0:00 to 12:00 on November 5 and the period of sea wind weakening from 12:00 on November 6 to 5:00 on November 7. The blue and red arrows represent the trends of the peak positions of LPDF and SPDF

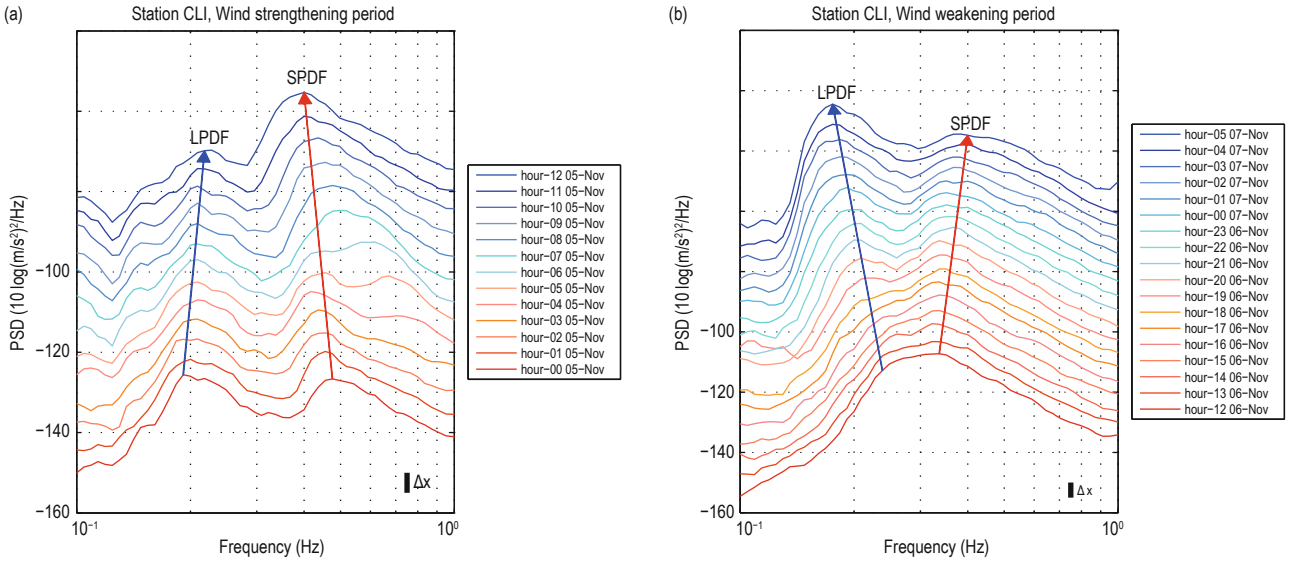

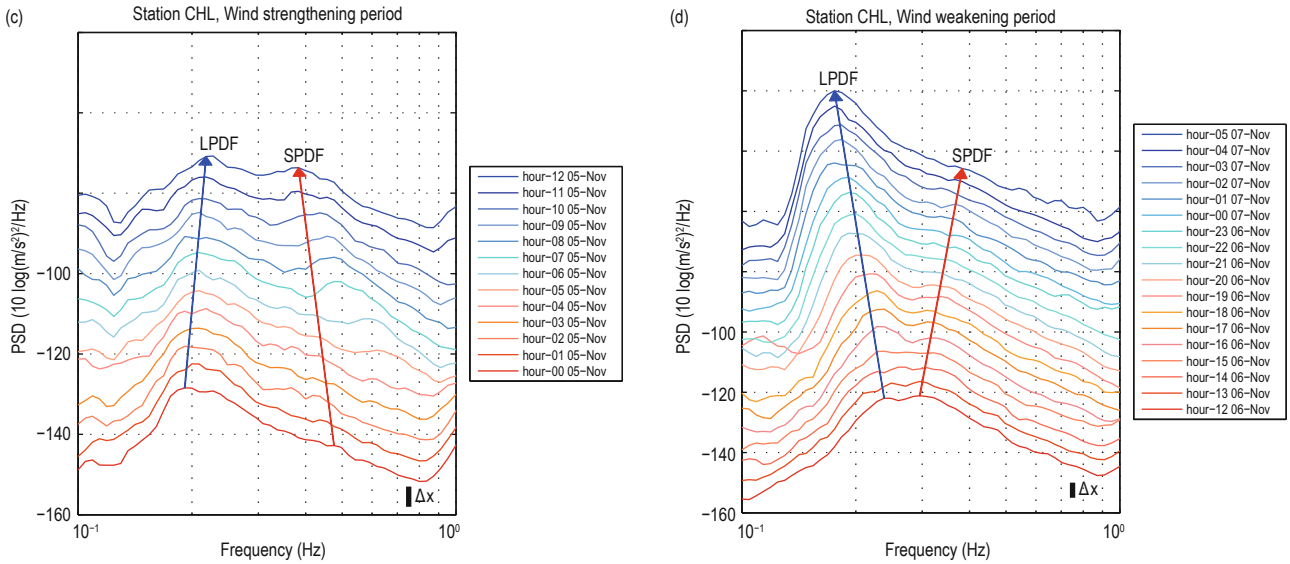

Figure 4. Variation in seismic noise PSD curves of stations (a) CLI and (c) CHL during the wind strengthening period from 0:00 to 12:00 on November 5 and of stations (b) CLI and (d) CHL during the wind weakening period from 12:00 on November 6 to 5:00 on November 7. The first curves from the bottom correspond to the true PSD values, and the other curves are sequentially shifted upward Δx (marked at the right bottom of each figure). The blue and red arrows represent the trends of the peak positions of LPDF and SPDF microseisms over time, respectively.

microseisms over time, respectively. According to Figures 4a and 4c, both LPDF and SPDF microseisms are at lower levels at 0:00 on November 5 when the sea wind is weak. As the sea wind strengthens, the energy of SPDF microseisms strengthens, and the dominant frequencies decrease gradually, whereas the energy of LPDF microseisms exhibits a slight weakening trend and the dominant frequencies gradually increase, which is consistent with the process of the growth of wind waves and the decay of swells. According to Figures 4b and 4d, during the process of sea wind weakening, significant alternating changes in SPDF and LPDF microseisms are observed. In other words, the energy of SPDF microseisms weakens and the dominant frequencies increase, whereas the energy of LPDF microseisms strengthens and the dominant frequencies decrease gradually, which is consistent with the process of the decay of wind waves and the growth of swells.

On the basis of the above phenomena and combined with the generation mechanisms and characteristics of waves in the Bohai Sea, we conclude that SPDF microseisms are primarily generated by irregular wind waves during strong offshore wind periods, with a broad frequency band distributed in the range of 0.2–1 Hz; LPDF microseisms are primarily generated by regular swells during periods of sea wind weakening, with frequencies concentrated between 0.15 and 0.3 Hz.

PSD analysis in terms of spatial dimensions

Figures 5 and 6 show the comparison of the time-domain waveforms and PSD curves between stations CLI and CHL during the strong wind period at 12:00 on November 6 and the weak wind period at 5:00 on November 7. Figures 5a and 5b show the time-domain waveforms of stations CLI and CHL during the strong wind period, respectively. Compared with station CLI, station CHL, which is further away from the coastline, exhibits a significant decrease in waveform frequencies and energy during the strong wind period, mainly because of the attenuation of high-frequency components of SPDF microseisms during propagation. Notably, compared with Figure 5c, Figure 5d shows no significant change in waveform frequencies during the weak wind period; however, the energy has a certain enhancement. As shown in Figure 6, the noise levels of the two stations are quantitatively analyzed using PSD curves. The blue arrows represent the LPDF microseism peaks during the weak wind period, and the red arrows represent the SPDF microseism peaks during the strong wind period. The values marked in parentheses represent the dominant frequencies and PSD peak values of LPDF and SPDF microseisms. The comparison results are

consistent with the conclusion in Figure 5.

To further validate the spatial variation regularity of the secondary microseisms generated in the Bohai Sea and analyze their impact on seismic noise, we used the method shown in Figure 6 to extract the PSD peak values of SPDF microseisms during the strong wind period at 12:00 on November 6 and the PSD peak values of LPDF microseisms during the weak wind period at 5:00 on November 7 recorded by 33 stations distributed according to Figure 1. The results are shown in Figure 7. Figure 7a illustrates the spatial distribution of the PSD peak values of SPDF microseisms in the northwest

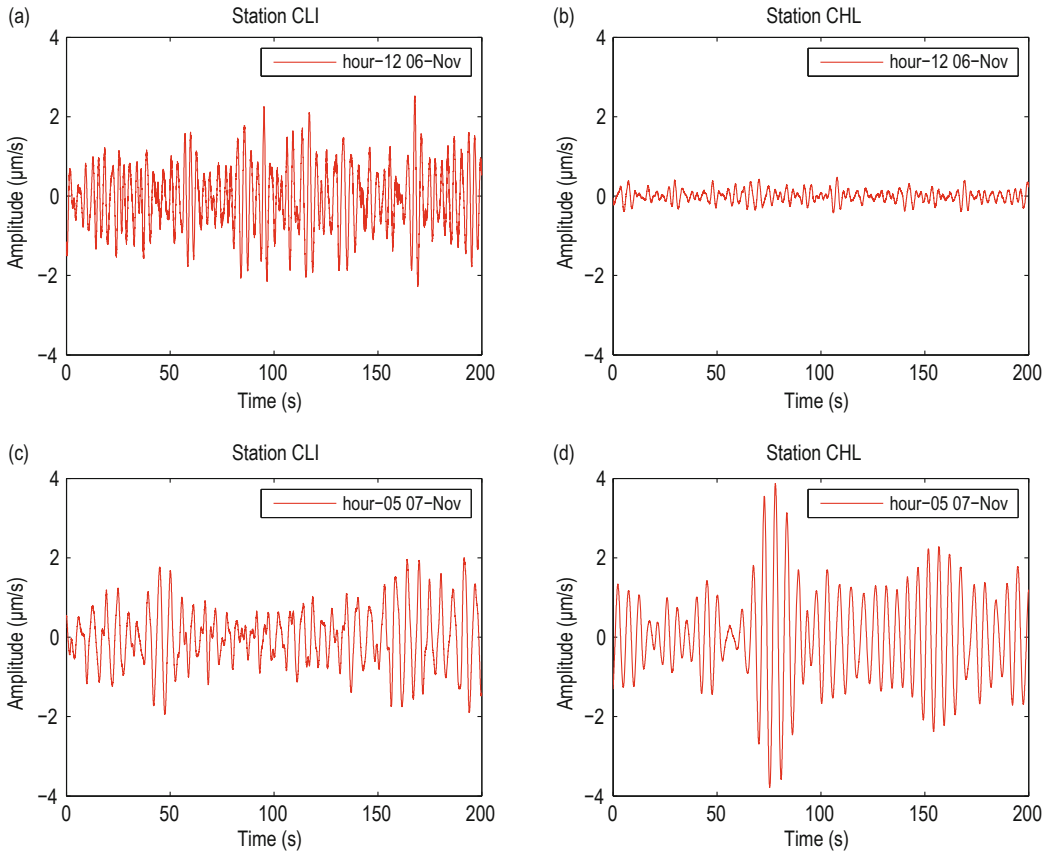

Figure 5. Time-domain waveforms of seismic noise. (a) and (b) show the time-domain waveforms of stations CLI and CHL at 12:00 on November 6, respectively; (c) and (d) show the time-domain waveforms of stations CLI and CHL at 5:00 on November 7, respectively. Only the first 200-s waveforms every hour are displayed.

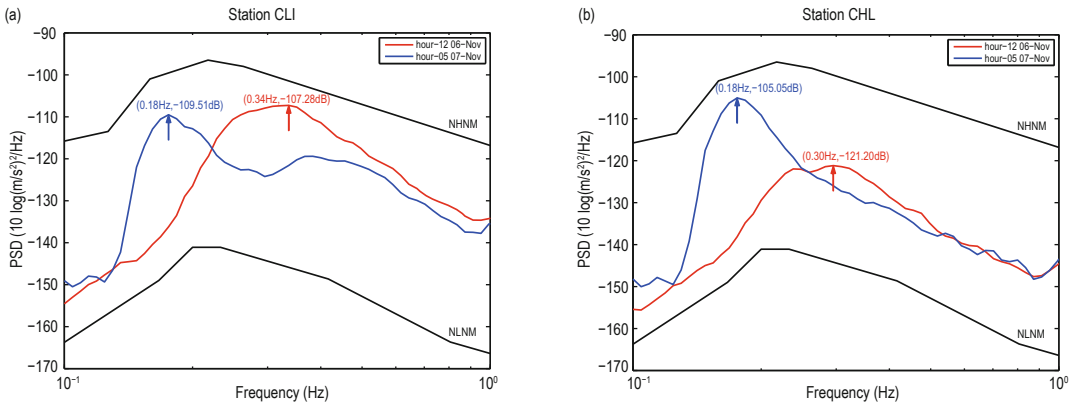

Figure 6. PSD curves of seismic noise of stations (a) CLI and (b) CHL at 12:00 on November 6 and 5:00 on November 7. The blue arrows represent the LPDF microseism peaks, and the red arrows represent the SPDF microseism peaks. The values marked in parentheses represent the dominant frequencies and PSD peak values of LPDF and SPDF microseisms. The two black curves represent Peterson's (1993) new high noise model (NHNM) and new low noise model (NLNM).

inland area of the Bohai Sea. The energy of SPDF microseisms is negatively correlated with the distance from the coastline, indicating that the energy of SPDF microseisms gradually attenuates during propagation inland. Figure 7b illustrates the spatial distribution of the PSD peak values of LPDF microseisms. In contrast, the LPDF microseism energy of some stations exhibits a certain enhancement as the distance from the coastline increases. Combined with Figure 1, it can be seen that the LPDF microseism energy corresponds well with the station elevations, and the energy is enhanced more quickly when the microseisms propagate along the path with higher elevations in the northern area, which indicates that LPDF microseisms with lower and concentrated frequency bands exhibit a certain site amplification effect when propagating in high-elevation areas. Many studies have shown that sedimentary basins and shallow and low-speed sedimentation have a significant amplification effect on microseisms between 0.1 and 1 Hz (Fu et al., 2023; Wan et al., 2024). The stations with a more obvious amplification phenomenon above the red dashed line shown in Figure 7b are mostly located in the Bashang region of the Hebei Province and southeastern Inner Mongolia Plateau, and the signals are concentrated between 0.15 and 3 Hz, as recorded by rock seismic stations. Thus, the amplification mechanisms need to be further investigated.

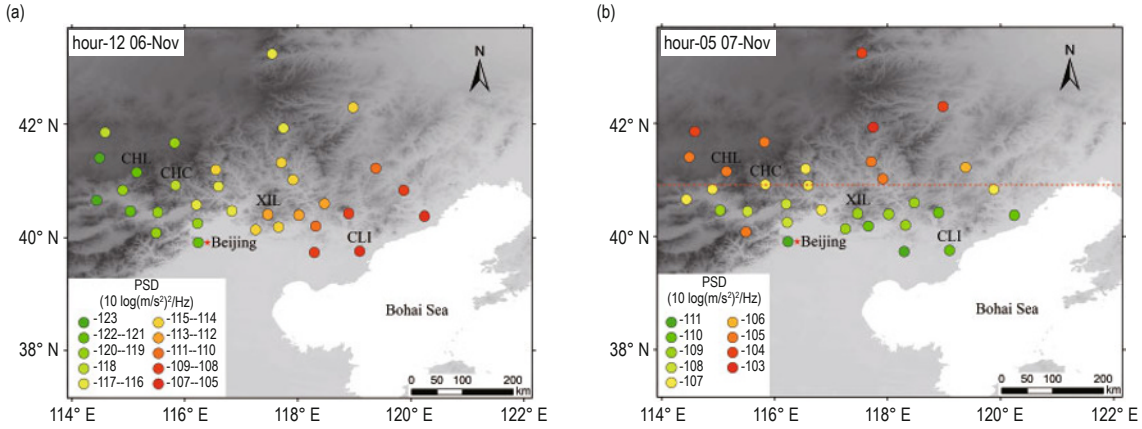

Figure 7. Spatial distribution of the PSD peak values of secondary microseisms in the northwest inland area of the Bohai Sea. (a) PSD peak values of SPDF microseisms recorded by 33 stations at 12:00 on November 6. (b) PSD peak values of LPDF microseisms recorded by 33 stations at 5:00 on November 7. The stations with a more obvious amplification phenomenon are located above the red dashed line.

PDF analysis on long-time scales

To further validate the applicability of the above theories to the region, consecutive observation data from stations CLI and CHL for four months from November 2023 to February 2024 were selected to calculate the PDF distribution of the PSD curves between 0.1 and 1 Hz (Figure 8). The seismic noise level of station CHL further away from the coastline is far below Peterson's (1993) NHNM, mainly due to the energy attenuation of SPDF microseisms during propagation. The black curves represent the typical values of seismic noise PSDs with the advantageous probabilities, and the typical value curves show an abrupt change at approximately 0.3 Hz. The LPDF microseisms dominate the probability distribution below 0.3 Hz, while the SPDF microseisms dominate above 0.3 Hz, and the probabilities are similar. The significant enhancement of SPDF microseism energy between 0.3 and 1 Hz is primarily related to the growth of wind waves during strong wind periods and is more obvious for station CLI, which is closer to the coastline. This phenomenon indicates that strong wind weather frequently occurs in the Bohai Sea and that the conclusions drawn from the observation data from November 3 to 7, 2023, are applicable on long-time scales.

From the PDF distribution of station CLI in Figure 8a, it can be seen that between 0.25 and 0.4 Hz, the microseism energy with advantageous probabilities shows a phenomenon of spanning at the same frequency. The higher energy part corresponds to the SPDF microseisms during strong sea wind periods, while the lower energy part corresponds to the LPDF microseisms during weak sea wind periods, and the probabilities are similar. This further indicates that the energy of SPDF

and LPDF microseisms exhibits alternating trends in the northwest area of the Bohai Sea. As shown in Figure 8b, for station CHL, which is located far from the coastline, the same phenomenon of energy spanning is also present. However, because of the substantial energy attenuation of SPDF microseisms, the secondary microseisms are dominated by LPDF microseisms.

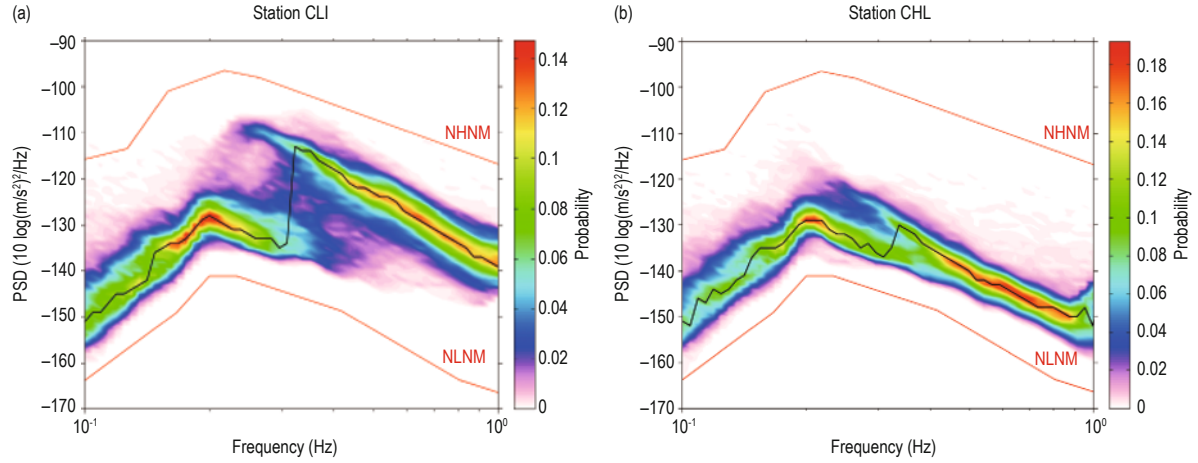

Figure 8. PDF distribution of PSD curves for seismic noise at stations (a) CLI and (b) CHL. The black curves represent the typical values of seismic noise PSDs with the advantageous probabilities. The two red curves represent NHNM and NLNM.

Conclusions

On the basis of previous studies, we further investigated the characteristics of secondary microseisms generated in the Bohai Sea and their impact on seismic noise. Based on the analysis of observation data from 33 broadband rock seismic stations in the northwest inland area of the Bohai Sea, new perspectives were proposed on the generation mechanisms and characteristics of SPDF and LPDF microseisms, combined with the special geographical location and wave characteristics of the Bohai Sea. The conclusions provide important supplements to the basic theory of secondary microseisms and preliminarily reveal the relationship between the atmosphere, ocean, and seismic noise.

The Bohai Sea belongs to the inland sea; however, SPDF and LPDF microseisms can still be observed in its northwest inland area, which presents significant alternating trends of strengthening and weakening with the process of sea wind action. SPDF microseisms are primarily generated by irregular wind waves during strong offshore wind periods, with a broad frequency band distributed in the range of 0.2–1 Hz, and the frequency and energy are related to the characteristics of the sea wind; LPDF microseisms are primarily generated by regular swells during periods of sea wind weakening, with a narrow frequency band concentrated between 0.15 and 0.3 Hz.

In terms of temporal dimensions, as the sea wind weakens, the energy of SPDF microseisms weakens, and the dominant frequencies increase, whereas the energy of LPDF microseisms strengthens and the dominant frequencies decrease, which is consistent with the process of the decay of wind waves and the growth of swells. In terms of spatial dimensions, as the microseisms propagate inland areas, the advantageous frequency band and energy of SPDF microseisms are reduced and attenuated significantly, respectively, whereas LPDF microseisms show no significant changes. And during propagation in high-elevation areas, LPDF microseisms exhibit a certain site amplification effect when the energy is strong. On the basis of the characteristics of secondary microseisms and their variation regularity with space and elevation, qualitative investigation of the instrument performance and parameter accuracy of the seismic network can be performed, and important theoretical references can be provided for regional seismic intensity assessment, seismic fortification, and geological and oceanographic research.

Based on the analysis of the PDF of seismic noise on long-time scales, for stations closer to the coastline, the energy of SPDF microseisms is higher and dominates in the noise models, which is related to the occurrence frequency and intensity of sea wind; for stations located far from the coastline, due to the significant energy attenuation of SPDF microseisms, the secondary microseisms are dominated by LPDF microseisms. The

focus of our next study will be on establishing suitable seismic noise models for the region, considering factors such as the distances between stations and coastlines, elevations, sea wind processes, and amplification mechanisms of LPDF microseisms.

Acknowledgments

We would like to acknowledge the reviewers for their constructive suggestions for the improvement of the manuscript. This study is supported by Earthquake Science and Technology Spark Program of China Earthquake Administration (No. XH2000Y), Local Standards Formulation and Revision Program of Hebei Province (No. FW202154), Earthquake Science and Technology Spark Program of Hebei Earthquake Agency (No. DZ2024112100002), and 2023 Seismological Data Sharing Project of China Earthquake Networks Center (Dataset Project).

References

Bromirski, P. D., Duennebier, F. K., and Stephen, R. A., 2005, Mid-ocean microseisms: Geochemistry, Geophysics, Geosystems, **6**(4), 1−19.

Chen, D. L., Lin, J. M., Ni, S. D., et al., 2018, Characteristics of seismic noise on ocean islands in Northwest Pacific and its oceanographic interpretation: Chinese Journal of Geophysics, **61**(1), 230−241.

Cupillard, P., and Capdeville, Y., 2010, On the amplitude of surface waves obtained by noise correlation and the capability to recover the attenuation: A numerical approach: Geophysical Journal International, **181**(3), 1687−1700.

Fu, L., Xie, J. J., Chen, S., et al., 2023, Analysis of site amplification coefficient characteristics of Sichuan and its application in strong ground-motion simulation: A case study of 2022 Lushan Ms6.1 earthquake: Chinese Journal of Geophysics, **66**(7), 2933−2950.

Ge, H. K., Chen, H. C., Ouyang, B., et al., 2013, Transportable seismometer response to seismic noise in vault: Chinese Journal of Geophysics, **56**(3), 857−868.

Guo, P. F., Shi, P., Wang, H., et al., 1997, A new criterion between wind wave and swell wave−−by mixed wave composition factors and its application to the South China Sea: Journal of Ocean University of Qingdao, **27**(2), 131−137.

Guo, Y. J., An, Q., Bao, Y., et al., 2023, Background noise characteristics of seismological observation and strong earthquake of early warning reference stations in eastern Inner Mongolia: Journal of Geodesy and Geodynamics, **43**(7), 761−766.

Hasselmann, K., 1963, A statistical analysis of the generation of microseisms: Reviews of Geophysics, **1**(2), 177−210.

Hwang, P. A., Ocampo-Torres, F. J., and García-Nava, H., 2012, Wind sea and swell separation of 1D wave spectrum by a spectrum integration method: Journal of Atmospheric and Oceanic Technology, **29**(1), 116−128.

Koper, K. D., and Burlacu, R., 2015, The fine structure of double-frequency microseisms recorded by seismometers in North America: Journal of Geophysical Research: Solid Earth, **120**(3), 1677−1691.

Lay, T., Aster, R. C., Forsyth, D. W., et al., 2009, Seismological grand challenges in understanding earth's dynamic systems: Report to the National Science Foundation, IRIS Consortium, 1−76.

Lepore, S., and Grad, M., 2018, Analysis of the primary and secondary microseisms in the wavefield of the ambient noise recorded in northern Poland: Acta Geophysica, **66**(C5), 915−929.

Lepore, S., and Grad, M., 2020, Relation between ocean wave activity and wavefield of the ambient noise recorded in northern Poland: Journal of Seismology, **24**(6), 1075−1094.

Li, X. J., Yang, D. K., Xie J. B., et al., 2015, Applicability of the Welch method for examining self-noise level parameters for broadband seismometers: Geodesy and Geodynamics, **6**(3), 233−239.

Lin, B. H., Jin, X., Huang, L. Z., et al., 2020, Quantitative assessment of background noise levels of seismic stations and their application in air-gun source detection: China Earthquake Engineering Journal, **42**(6), 1555−1564.

Longuet-Higgins, M. S., 1950, A theory of the origin of microseisms: Philosophical Transactions of the Royal Society of London. Series A, Mathematical and Physical Sciences, **243**(857), 1−35.

McNamara, D. E., and Buland, R. P., 2004, Ambient Noise Levels in the Continental United States: Bulletin of the Seismological Society of America, **94**(4), 1517−1527.

Niu, S. K., Yin, L., and Gai, M. L., 1999, Calculating and analyzing of the wind wave in the south area of Bohai: Coastal Engineering, **18**(3), 13−16.

Peterson, J. R., 1993, Observations and modeling of seismic background noise: U.S. Geological Survey, Open-File Report 93−322, 1−94.

Sleeman, R., van Wettum, A., and Trampert, J., 2006, Three-channel correlation analysis: a new technique to measure instrumental noise of digitizers and seismic sensors: Bulletin of the Seismological Society of America, **96**(1), 258−271.

Sleeman, R., and Vila, J., 2007, Towards an automated quality control manager for the Virtual European Broadband Seismograph Network (VEBSN): Orfeus Newsletter, **7**(1), 1−12.

Sorrells, G. G., and Douze, E. J., 1974, A preliminary report on infrasonic waves as a source of long-period seismic noise: Journal of Geophysical Research, **79**(32), 4908−4917.

Sun, L. C., 1991, Analysis of wave Characteristics of the west offshore area of the Bohai Bay: Journal of Oceanography of Huanghai & Bohai Seas, **9**(3), 50−58.

Wan, W. T., Chen, C., Wang, Y., et al., 2024, Comparative analysis of surface and deep underground seismic ambient noise: Chinese Journal of Geophysics, **67**(2), 793−808.

Wang, B. X., Chang, R. F., and Wang, Y. F., 1990, Criteria of differentiating swell from wind waves: Journal of Oceanography of Huanghai & Bohai Seas, **8**(1), 16−24.

Wang, W. T., Ni, S. D., and Wang, B. S., 2011, New advances in application of ambient noise interferometry: Earthquake Research in China, **27**(1), 1−13.

Wei, J., Hao, H. T., Yang, J. L., et al., 2020, Detecting DF microseisms by gPhone gravimeter on Fuzhou seismic station during Dujuan typhoon: Progress in Geophysics, **35**(6), 2107−2115.

Wei, J., Lü P. J., Hao, H. T., et al., 2022, Study on the anomalies of the double frequency microseisms before Yingcheng Ms4.9 earthquake: Journal of Geodesy and Geodynamics, **42**(1), 88−95.

Welch, P. D., 1967, The use of fast Fourier transform for the estimation of power spectra: a method based on time averaging over short, modified periodograms: IEEE Transactions on Audio and Electroacoustics, **15**(2), 70−73.

Wiegel, R. L., 1960, Wind waves and swell: Coastal Engineering Proceedings, **1**(7), 1−40.

Wu, J. P., Ouyang, B., Wang, W. L., et al., 2012, Ambient noise level of North China from temporary seismic array: Acta Seismologica Sinica, **34**(6), 818−829.

Xiao, H., Xue, M., Yang T., et al., 2018, The characteristics of microseisms in South China Sea: results from a combined data set of OBSs, broadband land seismic stations, and a global wave height model: Journal of Geophysical Research: Solid Earth, **123**(5), 3923−3942.

Xie, J. T., Lin, L. P., Chen L., et al., 2018, The program of probability density function of power spectral density curves from seismic noise of a station based on Matlab: Seismological and Geomagnetic Observation and Research, **39**(2), 84−89.

Xu, W. W., and Yuan, S. Y., 2019, A case study of seismograph self-noise test from Trillium 120QA seismometer and Reftek 130 data logger: Journal of Seismology, **23**(4), 1347−1355.

Yang, Q. L., Hao, C. Y., and Tian, X., 2019, Ambient noise analysis by the technology of PSD and PDF in Hotan Seismic Array: Chinese Journal of Geophysics, **62**(7), 2591−2606.

Yin, W. Y., and Zhang, Y. N., 2006, Statistical analysis of wind and wave features at Bohai straits: Journal of Dalian Maritime University, **32**(4), 84−88.

Zheng, L. L., Lin, J. M., Ni, S. D., et al., 2017, Characteristics and generation mechanisms of double frequency microseisms generated by typhoons: Chinese Journal of Geophysics, **60**(1), 187−197.

Yin Kang-Da graduated from Hebei University of Technology with a master's degree in 2013. He currently works at the Hebei Earthquake Agency and Hebei Hongshan National Observatory on Thick Sediments and Seismic Hazards, whose main research direction is seismic observation technology.

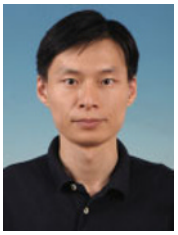

Email: yinkangda@126.com